COMMUNICATION

Cu[II]-mediated Ultra-efficient Electrooxidation of Glucose

Weiran Zheng, Yong Li, Chui-Shan Tsang, Liangsheng Hu, Mengjie Liu, Bolong Huang, Lawrence Yoon Suk Lee,* and Kwok-Yin Wong*

Abstract: Electrooxidation of glucose represents an economic conversion of biomass and has gained global interests for applications in fuel cells and sensors. Herein, we report a new, simple, and highly efficient method of glucose electrooxidation without involving any sophisticated electrode modification with biocatalysts or nanostructures. μM level Cu ions are added to coordinate with glucose in alkaline electrolyte. The coordinated glucose is oxidized by electrochemically generated Cu[III] with excellent conversion efficiency (TOF = 18.7 s^{-1}) and ultra‐high sensitivity (1,814 mA M^{-1} cm^{-2}) under mild conditions. Both experimental and theoretical investigations show that the Cu[II]-glucose plays a critical role in such high efficiency, which significantly reduces the oxidation potential and avoids catalyst poisoning. Our electrocatalytic system delivers remarkable atomic efficiency with high stability, thus offers great potential for applications in fuel cell and sensor design at low cost.

Catalytic biomass transformation, in particular glucose oxidation, has attracted wide interests in the last few decades for many potential applications such as generation of energy,[1] alternate source for chemical products,[2] and biomedical devices.[3] A fast and stable system has long been desired for such transformation to realize renewable and sustainable power supply in glucose fuel cell, especially for implantable biomedical devices, as well as quick and precise detection of glucose. Many methods including biochemical process,[4] hydrothermal catalysis,[2] and electrochemical catalysis[5] have been explored to achieve highly efficient, selective, and stable conversion of glucose. Apart from the enzyme, noble metals, such as Au,[2,6] Pt,[7,8] and Pd[7] have been commonly adopted as a catalyst for glucose oxidation. However, the involvement of enzyme and noble-metal catalyst raises problems of long-term stability and high cost. It is also very common that both biocatalysis and hydrothermal catalysis require certain temperature and oxygen pressure, which further complicates the system.[2,7]

Electrochemical catalysis offers a promising alternative for glucose oxidation. Since first developed decades ago, the glucose electrooxidation has become a critical reaction involved in many research areas, including fuel cell[3,9] and non-enzymatic sensor.[5,10] Unlike hydrothermal catalytic processes, the electrochemical conversion of glucose is usually performed under mild conditions: room temperature and atmospheric oxygen pressure. Moreover, non-noble metals, such as Cu[11] and Ni,[12] are engaged as an electrocatalyst for glucose electrooxidation, further bringing down the cost.

So far, copper-based nanomaterials (Cu, CuO, Cu$_2$O, Cu(OH)$_2$, etc.) are among the most studied non-noble metal electrocatalysts because of their high activities.[13-15] Extensive efforts have been put in to increase the number of active sites and the conductivity of nanomaterials to gain high reactivity and sensitivity towards glucose. The use of carbon nanotube and graphene as catalyst supports and the alteration of nanostructure shapes are good examples.[14,16-18] Unfortunately, such nanomaterials share similar problems, for instance, long-term stability under certain potential and surface poisoning by adsorbed products. Such disadvantages usually make the conversion of glucose less efficient than the hydrothermal catalytic process. Moreover, the preparation of nanomaterials often requires careful morphology control and electrode modification, which voids the advantages of electrocatalysis in its simplicity and cost.

To achieve the rational design of highly efficient electrocatalyst, the mechanism of glucose electrooxidation *via* Cu-based electrocatalysts needs to be thoroughly understood. It is commonly accepted that in alkaline solutions, the surface Cu species are oxidized first to Cu[III] species,[19,20] frequently referred as CuOOH or CuO$_2^-$ *in situ* formed on the surface, and these Cu[III] species act as an active oxidizer for glucose.[21-23] It means the current signal is only associated with the rate of Cu[II] oxidation (electron transfer), and the produced Cu[III] species further reacts with adsorbed glucose (redox reaction). Although electrochemically produced Cu[III] was evident mostly in cyclic voltammograms (CVs),[19,20] the mechanism of its reduction/regeneration in alkaline solution has never been demonstrated despite its well-known high activity in organometallic chemistry.[24,25] A very recent study by Deng *et al*. reported the *in situ* Raman spectroscopic observation of Cu[III] oxides produced by electrooxidation of Cu(OH)$_2$ or CuO which serve as an active species for oxygen evolution in KOH solution. The soluble Cu[III] oxides were rather unstable and could rapidly react with OH$^-$ to produce O$_2$.[26]

Since only the surface Cu[II] species that could be oxidized to Cu[III] serves as 'real' active sites,[22] it is reasonable to think of using only Cu ion (Cu[II]) for electrocatalysis. By doing so, one can save the effort of preparing Cu nanostructures where the majority of bulk Cu atoms are not engaged as active sites, achieving high atomic efficiency even at much lower Cu concentrations. Also, surface poisoning can be bypassed because the reactions on electrode only involve soluble Cu[II] and Cu[III] species.[20] Without the need for nanomaterial or enzyme, the process of glucose electrooxidation could be much simplified and thus cheaper. However, no one has studied nor proposed such a system yet.

In this paper, we present a new and straightforward way for glucose electrooxidation using μM level Cu[II] ion as a catalyst without any electrode modification nor specific nanomaterial design. The mechanism is thoroughly studied by combining cyclic voltammetry (CV), NMR, *in situ* electrochemical UV-Vis spectroscopy, and theoretical calculations. Such system shows not only comparable activities (turnover frequency, TOF) with hydrothermal catalysis but also one of the highest sensitivity values among all other electrocatalysts reported for glucose sensing to date. Moreover, in addition to high stability, the reaction activity can be tuned by altering the solution pH, potential, and surface area, making it a general and cost-effective method for the conversion of glucose towards numerous potential applications.

*   W.Z.; Y.L.; C.-S.T; L.H.; M.L.; B.H; L.Y.S.L.; K.-Y.W;
    Department of Applied Biology and Chemical Technology and the State Key Laboratory of Chirosciences
    The Hong Kong Polytechnic University
    Hung Hom, Kowloon, Hong Kong SAR, China
    E-mail: lawrence.ys.lee@polyu.edu.hk (L.Y.S. Lee);
    kwok-yin.wong@polyu.edu.hk (K.-Y. Wong)

    Supporting information for this article is given via a link at the end of the document.

Firstly, it is important to understand the chemical/electrochemical behaviors of Cu^{II} in alkaline solution. Cu^{II} ions in 0.1 M NaOH are known to undergo the following reactions (1) ~ (3).[27] The soluble $Cu(OH)_3^-$ (or $HCuO_2^-$) is the major species at pH > 12 (**Figure S1**).
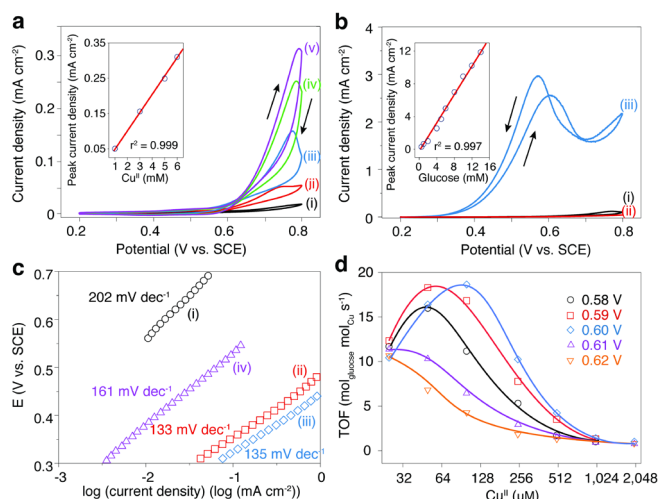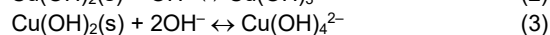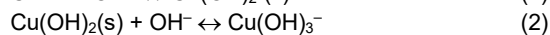
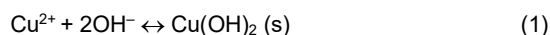$$Cu^{2+} + 2OH^- \leftrightarrow Cu(OH)_2 \text{ (s)} \tag{1}$$
$$Cu(OH)_2(s) + OH^- \leftrightarrow Cu(OH)_3^- \tag{2}$$
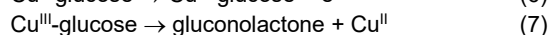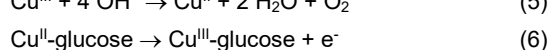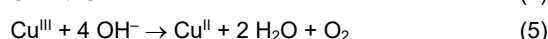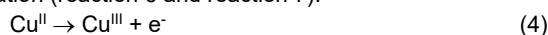$$Cu(OH)_2(s) + 2OH^- \leftrightarrow Cu(OH)_4^{2-} \tag{3}$$

Figure 1. a. CVs of bare GCE in 0.1 M NaOH solution containing Cu^{II} (**i**. 0 mM; **ii**. 1 mM; **iii**. 3 mM; **iv**. 5 mM; **v**. 6 mM). Inset is the plot of linear correlation between peak current density and Cu^{II} concentration. **b.** CVs of bare GCE in 0.1 M NaOH solution containing **i**. 4 mM Cu^{II}; **ii**. 4 mM glucose; **iii**. 4 mM Cu^{II} and 4 mM glucose. Inset is the linear correlation plot between peak current density and glucose concentration while Cu^{II} concentration is fixed at 4 mM. **c.** Corresponding Tafel plots of GCE in 0.1 M NaOH solution containing **i**. 4 mM Cu^{II}; **ii**. 4 mM Cu^{II} and 4 mM glucose; **iii**. 4 mM Cu^{II} and 6 mM glucose; **iv**. 2 mM Cu^{II} and 6 mM glucose. **d.** Turnover frequency (TOF) of glucose at the various potential on GCE normalized by total Cu^{II} concentration, calculated based on the charge input during 30 mins of electrooxidation, glucose concentration is 2 M, NaOH concentration is 2 M.

Figure 1a shows the CVs of glassy carbon electrode (GCE) in 0.1 M NaOH solution with various Cu^{II} concentrations. An oxidation current appears in the positive scan from ~0.55 V (*vs*. saturated calomel electrode (SCE), unless stated otherwise) and reaches a peak at 0.75 – 0.79 V, which is absent from Cu^{II}-free electrolyte. This current is assigned to the Cu^{II} to Cu^{III} oxidation (reaction 4).[28-31] The corresponding reduction peak is missing because Cu^{III} is quite reactive and would be chemically reduced back to Cu^{II} species (CuO or $Cu(OH)_2$, reaction 5).[22,26,31] The excellent linear correlation between peak current density and Cu^{II} concentration indicates that the Cu^{II} species oxidized to Cu^{III} is soluble ($Cu(OH)_x^{y-}$ species). No other oxidation states of Cu within the potential range is evident. (**Figure S2**)

The highly reactive Cu^{III} was further studied for glucose oxidation. **Figure 1b** compares the CVs of glucose with and without Cu^{II}. In the absence of Cu^{II}, no glucose electrooxidation is visible. After adding 4 mM Cu^{II}, however, the current rises dramatically from 0.35 V and reaches its maximum at 0.60 and 0.56 V during the anodic and cathodic scan, respectively. Considering that Cu^{II} shows negligible current in the absence of glucose, such hikes in current indicate a remarkable acceleration of the Cu^{II} electrooxidation (150 times greater) promoted by glucose. It is also noted that the oxidation potential for Cu^{II} is significantly lower

with glucose present (0.32 V *vs*. 0.55 V), suggesting that Cu^{II} oxidation may take a different path involving both Cu^{II} and glucose (reaction 6). Moreover, instead of reacting with OH^- (reaction 5),[26] Cu^{III} could take a much quicker (higher current) path *via* glucose oxidation (reaction 6 and reaction 7).

$$Cu^{II} \rightarrow Cu^{III} + e^- \tag{4}$$
$$Cu^{III} + 4\ OH^- \rightarrow Cu^{II} + 2\ H_2O + O_2 \tag{5}$$
$$Cu^{II}\text{-glucose} \rightarrow Cu^{III}\text{-glucose} + e^- \tag{6}$$
$$Cu^{III}\text{-glucose} \rightarrow \text{gluconolactone} + Cu^{II} \tag{7}$$

Altering the relative concentrations of Cu^{II} and glucose can provide more details of such promoting effect. With a fixed concentration of Cu^{II} (4 mM, **Figure S3**), the oxidation peak current increases linearly with glucose concentration (inset in **Figure 1b**). Apparently, the electrooxidation rate of Cu^{II} is further promoted by higher concentration of glucose. The peak potential gradually shifts from 0.57 to 0.72 V as the glucose concentration increases from 0.5 to 14 mM, indicating the mass transfer of glucose became rate limiting. In the opposite case where the various amount of Cu^{II} are used with 6 mM glucose, a similar increase in the oxidation peak is observed at 0.62 V without peak shifting (**Figure S4**). This implies that catalytic current is controlled by surface electron transfer rather than mass transfer under such conditions.

The reaction overpotential is shown in the Tafel plot of GCE (**Figure 1c**) in various electrolytes. It suggests that the presence of glucose significantly lowers the overpotential for Cu^{II} oxidation. With glucose present, the overpotentials are similar regardless the concentration of Cu^{II} and glucose (linear range starts from 0.3 V). Higher Cu^{II} concentration seems to enhance the reaction activity, as supported by more gentle slopes in Tafel plot. Higher glucose concentration, on the other hand, also increases current density, but the reaction rate (Tafel slope) of Cu oxidation remains similar.

The atomic efficiency of the Cu^{II} catalyst was studied at different Cu^{II} concentrations and applied potentials at room temperature. As plotted in **Figure 1d**, the TOF value exhibits a strong dependency on Cu^{II} concentration and applied potential. Because the oxidation of Cu^{II} on GCE involves both solid and liquid phases, we use the total Cu^{II} concentration for TOF calculation for simplicity. Within the studied Cu^{II} concentration range (0.025 to 2 mM), the TOF value increases first and reaches the maximum when potential is around 0.59 V. Possibly, the electrode surface is not saturated for Cu^{II} oxidation at low Cu concentrations. Once saturated, the increment of Cu^{II} concentration contributes less to the Cu^{III} production. With potential higher than 0.60 V, the TOF drops with higher Cu^{II} concentrations. The highest TOF value is 18.7 s^{-1} with 0.1 mM of Cu^{II} at 0.60 V, which is comparable with the previously reported hydrothermal catalyst.[32] Such catalytic system also shows excellent stability (**Figure S5**) without any significant current density drop within 2 h of reaction at 0.6 V.

The electrolyte of glucose electrooxidation was analyzed using NMR (**Figure S6**). Both gluconate and formate are evident as products, which is in good agreement with previous reports using Cu and Au electrodes.[33,34] Gluconate is found to be the dominant product at the initial stage of electrooxidation.

Table 1. Comparison of state-of-the-art Cu-based glucose sensors on modified GCE. All systems use 0.1 M NaOH as the electrolyte.

Electrocatalyst	E (*vs.* SCE)	Linear range	Detection limit (µM)[a]	Sensitivity (mA M^{-1} cm^{-2})	Ref.
CuO nanospheres	0.56 V	up to 2.55 mM	1	404	[35]
CuO nanofibers	0.40 V	up to 2.5 mM	0.8	431	[36]
CuO nanorods	0.56 V	up to 8 mM	4	371	[15]
CuO NPs/graphene oxide	0.66 V	2.8 µM to 2 mM	0.69	262	[16]
Cu NPs/graphene oxide/single wall nanotube	0.5 V	1 µM to 4.5 mM	0.34	930	[37]
CuO NPs/graphene	0.56 V	1 µM to 8 mM	1	1065	[38]
Cu^{2+}(1 mM)	0.6 V	0.5 µM to 10 mM	0.5	614	this work
Cu^{2+}(1 mM)/activated carbon (100 µg)	0.6 V	0.4 µM to 10 mM	0.2	1627	this work
Cu^{2+}(1 mM)/activated carbon (50 µg)[b]	0.6 V	0.4 µM to 10 mM	0.3	1814	this work

[a] Signal/noise ratio is 3. [b] Using 0.01 M NaOH solution.

The sensitivity (current response to glucose addition) is another key factor for evaluating glucose electrocatalysts since glucose sensor is one of the main fields of glucose oxidation.[39] We further compared our Cu^{II} catalyst with other state-of-the-art Cu-based electrocatalysts. For a given potential, there is an optimal Cu^{II} concentration for the highest sensitivity: 445, 523, and 614 mA M^{-1} cm^{-2} for 0.1 mM at 0.58 V, 0.15 mM at 0.59 V, and 1.0 mM at 0.60 V, respectively. (**Figure S7**) These sensitivity values based on our simple Cu^{II}-GCE system are among the best electrocatalysts to date, as shown in **Table 1**. For instance, a glucose sensor made of well-designed CuO nanomaterials has a sensitivity of ~400 mA M^{-1} cm^{-2} (0.6 V *vs.* SCE).[15,35]

By altering the reaction conditions (electrode surface area, pH, *etc.*), the activity (sensitivity) can be further improved. To increase electrochemical surface area, GCE is modified with activated carbon (AC) that is porous microcrystalline, non-graphitic form of carbon, and the results are shown in **Figure 2**. At a given Cu^{II} concentration, the sensitivity improves with larger amount of AC (**Figure 2a**), showing a linear correlation with the areal capacitance of GCE (**Figure S8**) up to 50 µg AC loading. It is reasonable that higher AC loading enriches active sites for Cu^{II} to Cu^{III} oxidation. The sensitivity reaches up to 1,612 mA M^{-1} cm^{-2} with higher Cu^{II} concentration, but levels off once Cu^{II} concentration exceeds 0.1 mM. It is believed that the electron transfer sites for Cu^{II} to Cu^{III} transition are saturated, which limits the current density.

The presence of OH$^-$ is critical to Cu^{II} electrooxidation.[26] The effect of OH$^-$ concentration on the sensitivity of glucose sensing is studied. **Figure 2c** shows the amperometric response of Nafion (0.25 wt%)-AC modified GCE to 0.1 mM glucose, and the calculated sensitivity is shown in **Figure 2d**. It is found that high sensitivity (> 1000 mA M^{-1} cm^{-2}) can only be obtained within a narrow pH window (11.6 – 13.1). A possible reason is that the concentration of Cu(OH)$_x^{y-}$ is relatively low at lower pH (<11.6), resulting in the slow rate of Cu^{II} electrooxidation to Cu^{III}. At higher pH (>13.1), a high concentration of OH$^-$ reacts with Cu^{III} and produces CuO, competing with glucose. The maximum sensitivity of 1,814 mA M^{-1} cm^{-2} is obtained at pH = 12 with Cu^{II} concentration of 1 mM on GCE coated with 50 µg AC. It is also found that short response time can be achieved at higher pH.
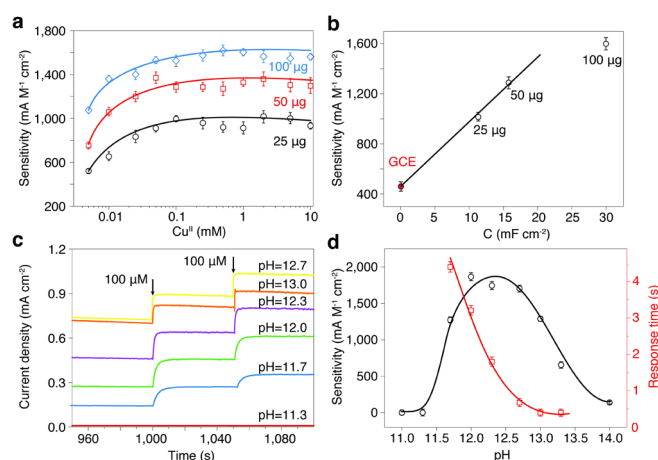

Figure 2. a. Sensitivity to glucose using Nafion-AC (25 µg, 50 µg, and 100 µg) modified GCE with different Cu^{II} concentrations in 0.1 M NaOH. **b.** Correlation between areal capacitance (C) and sensitivity. **c.** Amperometric response on Nafion-AC (50 µg) modified GCE at various pH. Each injection causes 0.1 mM changes of glucose concentration. Cu^{II} concentration is 1 mM. **d.** Sensitivity and response time *vs.* pH on Nafion-AC (50 µg) modified GCE. Applied potential is 0.6 V *vs.* SCE.

The detailed mechanism of such highly efficient catalytic system is studied by *in situ* electrochemical UV-Vis spectroscopy, electrochemical impedance spectroscopy, and density functional theory (DFT) calculations. The results of *in situ* electrochemical UV-Vis experiments are shown in **Figure 3a-c** (cell configuration shown in **Figure S9a**). The UV-Vis spectra of electrode surface in an electrolyte containing 0.4 mM Cu^{II} and 0, 0.1, or 0.4 mM glucose were measured within the selected potential range. **Figure 3a** shows two peaks at 282 and 362 nm when potential reaches 0.7 V during the positive scan, and they disappear at 0.5 V during the negative scan. These peaks are the characteristic peaks of CuO[40] (**Figure S10**). A steadily dropping trend at shorter wavelengths (220 to 250 nm) indicates the consumption of Cu(OH)$_x^{y-}$. After adding 0.1 mM glucose (**Figure 3b**), a new peak evolves at ~221 nm corresponding to the glucose. Higher glucose concentration (0.4 mM, **Figure 3c**) leads to the disappearance of CuO peaks. The trend of CuO production is illustrated in **Figure 3d** where UV-Vis absorbance at 362 nm is plotted against applied potential. Without glucose, the CuO peak rises from 0.55 V and culminates at ~0.75 V. During the negative scan, CuO peak

intensity decreases from 0.55 V, suggesting that majority of CuO is produced in the electrolyte, not adsorbed on the electrode. The CuO signal dramatically decreases with glucose addition and completely disappears after adding 0.4 mM glucose. It shows that the Cu^{III} to CuO reaction (reaction 5) is suppressed with glucose present, suggesting that Cu^{II} oxidation takes two paths with/without glucose: path 1 without glucose (reaction 4 and 5) and path 2 with glucose (reaction 6 and 7).

Figure 3e shows the Nyquist plots of 0.1 M NaOH solution containing Cu^{II} and glucose. Bare GCE shows the highest solution resistance. The addition of Cu^{II} and glucose reduces the resistance by ~165 and 240 Ω, respectively. When both Cu^{II} and glucose are present, the resistance drops dramatically by 622 Ω. It is possible that the coordination between glucose and Cu^{II} stabilizes Cu^{II} and prevents the formation of CuO or Cu(OH)$_2$. In 0.1 M NaOH, the resistance is determined by the diffusion rate of OH$^-$. With Cu^{II} present, the resistance drops due to Cu^{II} oxidation. Thus it is governed by the diffusion of OH$^-$ and Cu^{II}. With glucose present, the plot shows semi-circle feature that indicates the adsorption/desorption of glucose. In the presence of both glucose and Cu^{II}, the semi-circle persists, and more importantly, resistance dramatically drops. The coupling of Cu^{II} and glucose oxidation results in a great acceleration for both Cu^{II} and glucose oxidation.

The possible mechanism of the glucose oxidation is presented in **Figure 4a**. As suggested by NMR spectra (**Figure S11**), in NaOH
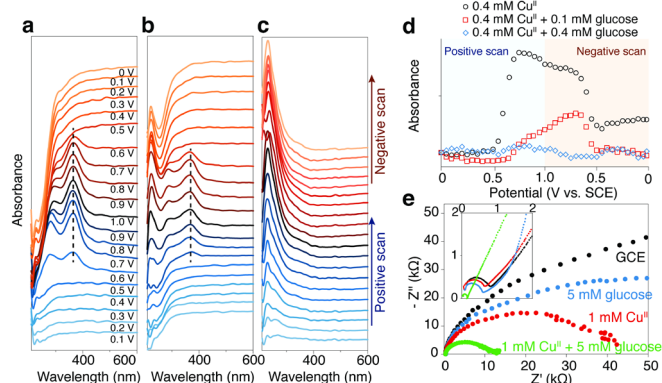

Figure 3. *in situ* electrochemical UV-Vis spectra of 0.4 mM Cu^{II} in 0.1 M NaOH with **a.** no glucose, **b.** 0.1 mM glucose, and **c.** 0.4 mM glucose. The spectra of first positive scan and first negative scan are shown, and the spectrum at 0 V (positive scan) is used as background. **d.** The absorbance at 362 nm as a function of applied potential. **e.** Nyquist plots of GCE at 0.6 V in 0.1 M NaOH solution containing different species within 10 mHz to 1 MHz, inset is the Nyquist plots at high frequency (100 Hz to 1 MHz).

solution, glucose loses one proton on -OH group, forming negatively charged glucose (*glu*$^-$). Such glu$^-$ can coordinate with Cu^{II} ion *via* two adjacent O atoms to form a Cu^{II}-glucose complex (*Cu^{II}-glu*$^-$). The complex is further oxidized on GCE electrode, producing *Cu^{III}-glu*$^-$.
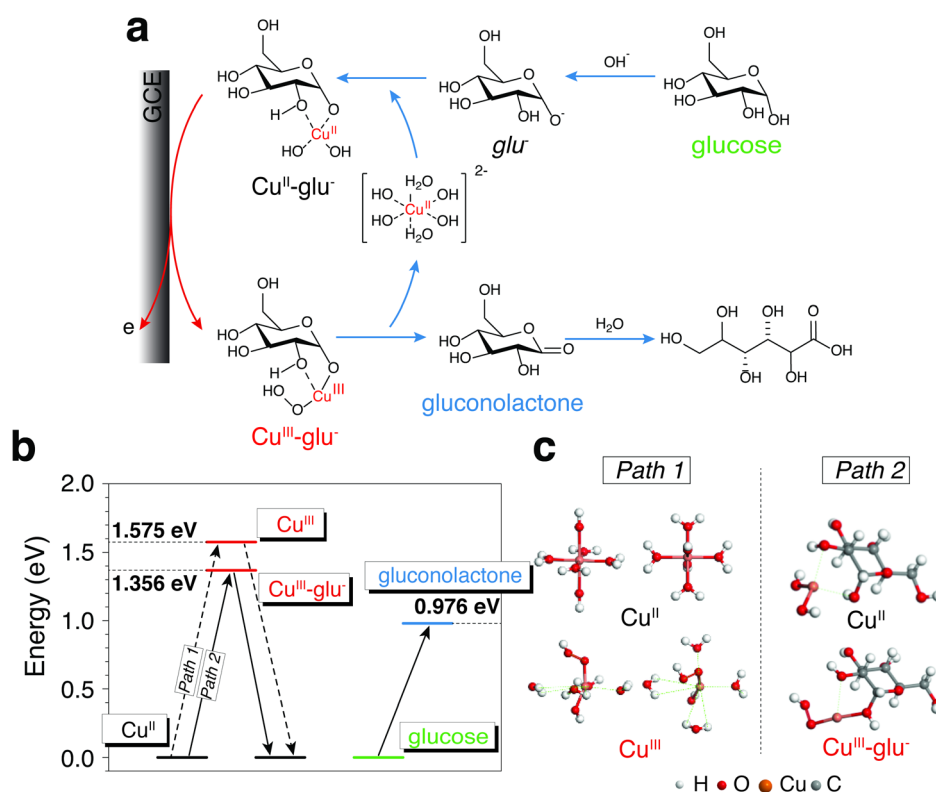

Figure 4. a. Mechanism of glucose oxidation *via* Cu^{II}-glucose coordination on GCE. **b.** Density functional theory (DFT) calculations of energy barriers of Cu^{II} oxidation without (path 1) and with (path 2) glucose. **c.** The structure of Cu^{II}, Cu^{III}, and *Cu^{III}-glu*$^-$ adopted for DFT calculations.

DFT calculations in **Figure 4b** shows the energy barrier of transformation from the ground state Cu^{II} to Cu^{III} complex (**Figure 4c**, path 1) is converged to 1.575 eV. With glucose present, Cu^{II}-glu^- complex is formed (**Figure 4c**, path 2). The oxidation of the Cu^{II}-glu^- to Cu^{III}-glu^- shows a significantly lower energy barrier, 1.356 eV, compared to that of path 1. Thus, path 2 would be favorable when both Cu^{II} and glucose are present. Regarding the chemical transition from glucose to gluconolactone, the formation energy is calculated to be 0.976 eV. The Cu^{III}-glu^- complex is highly unstable and would go through structural rearrangements, producing Cu^{II} and more stable gluconolactone.

For typical Cu-based nanomaterials, the surface Cu species would get oxidized first from Cu-OH to Cu-OOH species under applied potential. The adsorbed glucose then reacts with Cu-OOH, regenerating active sites and producing gluconolactone which desorbs from the catalyst surface.[5,16,23] Unlike such mechanism involving adsorption and desorption processes, our system engages Cu^{II} as active sites, which are homogeneously dispersed and coordinate with glucose, even without any potential applied. This Cu^{II}-glu^- complex is oxidized on the electrode surface and go through the process illustrated in **Figure 4a**. So, our Cu^{II} mediated catalysis process does not involve the adsorption/desorption processes of glucose on the catalyst surface, thus bypasses such rate limiting steps of glucose adsorption and gluconolactone desorption. Moreover, on nanomaterial modified electrode, the produced gluconolactone can adsorb and block the active sites on CuO, further lowering the activity and stability which can also be avoided in our system, as shown in **Figure 4a**, Cu^{II}-glu^- in double layer region is oxidized to Cu^{III}-glu^- on GCE. Such process only involves the coordination between Cu^{II} and glucose as well as charge transfer of Cu^{II}-glu^- species to the electrode surface, which is much faster than glucose adsorption/desorption (smaller resistance in **Figure 3e**). It is also noted that Cu^{II} can be produced locally by Cu^{III}-glu^-, further lowering the resistance.

To conclude, we demonstrated a highly efficient glucose oxidation method based on a simple Cu^{II} mediated electrocatalysis and studied its mechanism. Such high efficiency was attained *via* the Cu^{II}-glucose to Cu^{III}-glucose transition and the regeneration of Cu^{II} in double layer region. Combining *in situ* electrochemical spectroscopy results and DFT calculations, we found for the first time that this transition is kinetically and energetically favorable over Cu^{III} reduction by H_2O/OH$^-$. Such homogeneous catalytic system shows a high efficiency with TOF of 18.7 s^{-1} at room temperature on GCE. After simple optimizations, this Cu^{II} catalyst shows one of the highest activities among all reported Cu-based glucose electrocatalysts. The catalytic system shows high stability and excellent resistance to surface poisoning. It also requires very low Cu^{II} concentration without specifically designed Cu or CuO nanomaterials, thus considerably economically viable and environmental friendly. With much space for optimization (electrode surface area, pH, potential, *etc.*), such homogeneous Cu^{II} catalytic system has huge potential in industrial processes involving glucose electrooxidation.

[1] S. K. Chaudhuri, D. R. Lovley, *Nat. Biotechnol.* **2003**, *21*, 1229–1232.
[2] H. Zhang, N. Toshima, *Catal. Sci. Technol.* **2013**, *3*, 268–278.
[3] V. Oncescu, D. Erickson, *Sci. Rep.* **2013**, *3*, 159–156.
[4] F. Zhao, H. Li, Y. Jiang, X. Wang, X. Mu, *Green Chem.* **2014**, *16*, 2558–8.
[5] A. Brouzgou, P. Tsiakaras, *Top. Catal.* **2015**, *58*, 1311–1327.
[6] P. Qi, S. Chen, J. Chen, J. Zheng, X. Zheng, Y. Yuan, *ACS Catal.* **2015**, *5*, 2659–2670.
[7] I. V. Delidovich, O. P. Taran, L. G. Matvienko, A. N. Simonov, I. L. Simakova, A. N. Bobrovskaya, V. N. Parmon, *Catal. Lett.* **2010**, *140*, 14–21.
[8] B. S. D. G. V. Jechan Lee, *Green Chem.* **2016**, *18*, 3815–3822.
[9] L. Li, K. Scott, E. H. Yu, *J. Power Sources* **2013**, *221*, 1–5.
[10] M. M. Rahman, A. J. S. Ahammad, J.-H. Jin, S. J. Ahn, J.-J. Lee, *Sensors* **2010**, *10*, 4855–4886.
[11] C. Li, Y. Su, S. Zhang, X. Lv, H. Xia, Y. Wang, *Biosens. Bioelectron.* **2010**, *26*, 903–907.
[12] Y. Mu, D. Jia, Y. He, Y. Miao, H. Wu, *Biosens. Bioelectron.* **2011**, 2948–2952.
[13] Q. Xu, Y. Zhao, J. Z. Xu, J.-J. Zhu, *Sens. Actuators B: Chem* **2006**, *114*, 379–386.
[14] X. Zhang, G. Wang, X. Liu, J. Wu, M. Li, J. Gu, H. Liu, B. Fang, *J. Phys. Chem. C* **2008**, *112*, 16845–16849.
[15] X. Wang, C. Hu, H. Liu, G. Du, X. He, Y. Xi, *Sens. Actuators B: Chem* **2010**, *144*, 220–225.
[16] J. Song, L. Xu, C. Zhou, R. Xing, Q. Dai, D. Liu, H. Song, *ACS Appl. Mater. Interfaces* **2013**, *5*, 12928–12934.
[17] D. Jiang, Q. Liu, K. Wang, J. Qian, X. Dong, Z. Yang, X. Du, B. Qiu, *Biosens. Bioelectron.* **2014**, *54*, 273–278.
[18] J. Zhang, J. Ma, S. Zhang, W. Wang, Z. Chen, *Sens. Actuators B: Chem* **2015**, *211*, 385–391.
[19] J. S. Pap, Ł. Szyrwiel, *Comments Inorg. Chem.* **2016**, *37*, 1–19.
[20] M. Ohira, T. Sakai, M. Takeuchi, Y. Kobayashi, M. Tsuji, *Synth. Met.* **1987**, *18*, 347–352.
[21] N. Gagnon, W. B. Tolman, *Acc. Chem. Res.* **2015**, *48*, 2126–2131.
[22] J. M. Marioli, T. Kuwana, *Electrochim. Acta* **1992**, *37*, 1187–1197.
[23] A. Heller, B. Feldman, *Chem. Rev.* **2008**, *108*, 2482–2505.
[24] P. J. Donoghue, J. Tehranchi, C. J. Cramer, R. Sarangi, E. I. Solomon, W. B. Tolman, *J. Am. Chem. Soc.* **2011**, *133*, 17602–17605.
[25] D. Dhar, G. M. Yee, A. D. Spaeth, D. W. Boyce, H. Zhang, B. Dereli, C. J. Cramer, W. B. Tolman, *J. Am. Chem. Soc.* **2016**, *138*, 356–368.
[26] Y. Deng, A. D. Handoko, Y. Du, S. Xi, B. S. Yeo, *ACS Catal.* **2016**, *6*, 2473–2481.
[27] L. A. McDowell, H. L. Johnston, *J. Am. Chem. Soc.* **1936**, *58*, 2009–2014.
[28] *Lectures on Electrochemical Corrosion*, Springer US, **1973**.
[29] Z. J. Wu, Z. B. Zhang, L. S. Liu, *Electrochim. Acta* **1997**, *42*, 2719–2723.
[30] N. Torto, T. Ruzgas, L. Gorton, *J. Electroanal. Chem.* **1999**, *464*, 252–258.
[31] I. G. Casella, M. Gatta, *J. Electroanal. Chem.* **2000**, *494*, 12–20.
[32] T. Ishida, N. Kinoshita, H. Okatsu, T. Akita, T. Takei, M. Haruta, *Angew. Chem., Int. Ed.* **2008**, *47*, 9265–9268.
[33] M. Z. Luo, R. P. Baldwin, *J. Electroanal. Chem.* **1995**, *387*, 87–94.
[34] S. Dash, N. Munichandraiah, *J. Electrochem. Soc.* **2013**, *160*, H858–H865.
[35] E. Reitz, *Electroanalysis* **2008**, *20*, 2482–2486.
[36] W. Wang, L. Zhang, S. Tong, X. Li, W. Song, *Biosens. Bioelectron.* **2009**, *25*, 708–714.
[37] T. Yang, J. Xu, L. Lu, X. Zhu, Y. Gao, H. Xing, Y. Yu, W. Ding, Z. Liu, *J. Electroanal. Chem.* **2016**, *761*, 118–124.
[38] Y.-W. Hsu, T.-K. Hsu, C.-L. Sun, Y.-T. Nien, N.-W. Pu, M.-D. Ger, *Electrochim. Acta* **2012**, *82*, 152–157.
[39] C. Chen, Q. Xie, D. Yang, H. Xiao, Y. Fu, Y. Tan, S. Yao, *RSC Advances* **2013**, *3*, 4473–19.
[40] X. Y. Chen, H. Cui, P. Liu, G. W. Yang, *Appl. Phys. Lett.* **2007**, *90*, 183118–183120.

COMMUNICATION
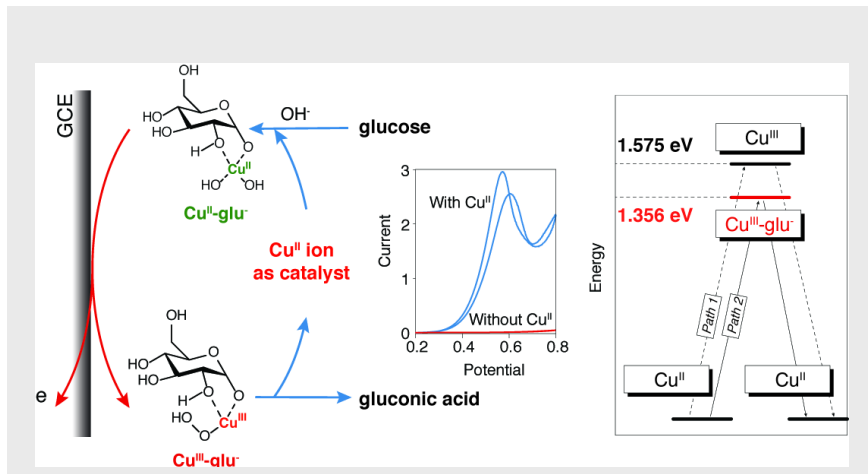
Weiran Zheng, Yong Li, Chui-Shan Tsang, Liangsheng Hu, Mengjie Liu, Bolong Huang, Lawrence Yoon Suk Lee* and Kwok-Yin Wong*

Page No. – Page No.

Cu^{II}-mediated Ultra-efficient Electrooxidation of Glucose